Geophys. J. Int. (1995) **120,** 775–782

α/β phase transition in quartz monitored using acoustic emissions

P. W. J. Glover,[1] P. Baud,[2] M. Darot,[2] P. G. Meredith,[1] S. A. Boon,[1] M. LeRavalec,[2] S. Zoussi[2] and T. Reuschlé[2]

[1]*Research School of Geological and Geophysical Sciences, University College London, Gower St, London* WC1E 6BT, *UK*
[2]*Laboratoire de Physique des Matériaux, Ecole et Observatoire de Physique du Globe,* 67084 *Strasbourg, France*

Accepted 1994 September 19. Received 1994 September 8; in original form 1994 June 3

SUMMARY

It is usually suggested that thermal cracking in a quartz-bearing rock results from the anomalously high volumetric expansion coefficients of quartz (e.g. Simmons & Cooper 1978). It has also been recognized that thermal expansion mismatch and mineral anisotropy contribute to thermal cracking in materials that consist of a polycrystalline aggregate composed of several anisotropic minerals even in the absence of a temperature gradient (Friedrich & Wong 1986). Experiments investigating thermal cracking in rocks commonly involve imaging and quantitative stereology of crack populations induced in rocks treated to various peak temperatures (e.g. Friedrich & Johnson 1978; Homand-Etienne & Troalan 1984; Atkinson, McDonald & Meredith 1984; Meredith & Atkinson 1985). Here we report on acoustic-emission experiments that monitor the process of thermal cracking as it occurs during heating, supported by measurements of crack surface area, pore-fluid permeability, porosity and surface conductivity carried out on rock samples treated to various peak temperatures. The acoustic-emission measurements show a strong peak of microcracking at the phase transition temperature for quartz (~573 °C) superimposed upon a background of microcracking due to thermal expansion. There is also a clear peak of microcracking at higher temperatures (~800 °C) that can be attributed to oxidation–dehydroxylation reactions of hornblende and chlorite. Measurements of fluid permeability, pore surface area, porosity and electrical conductivity, made on samples that have been heat treated to various maximum temperatures, show increases associated with a major episode of cracking in the 500–600 °C temperature range, indicating that the new cracks form a well-interconnected network. This has been confirmed by SEM and optical microscopy These results have implications for the electrical conductivity of the continental crust, providing a mechanism enabling the high pore-fluid connectivity needed to explain zones of high electrical conductivity at depth providing that cracks opened in this way remain open at the high pressures existing at depth. It should be recognized, however, that these measurements are limited in their direct application since they were obtained under initially dry conditions at laboratory pressures.

Key words: acoustic emissions, anisotropy, phase transitions, quartz, thermal cracking, thermal expansion.

1 EXPERIMENTAL

Acoustic-emission measurements were made by heating right-cylindrical samples of the unsaturated rock (40 mm long and 20 mm diameter) at 1 °C min^{-1} to various peak temperatures up to about 900 °C in air at laboratory pressures, whilst monitoring the thermally induced acoustic emissions they produced using a Locan AT analyser and a PZT piezoelectric transducer. The measurement set-up is shown in Fig. 1.

The rocks were obtained from several sources, which are summarized in Table 1. Samples were prepared by coring with a diamond-impregnated core drill and subsequently surface ground to ensure the ends were flat and parallel with a diamond-impregnated wheel. The samples were stored at 40 °C prior to use.

The acoustic-emission transducer was not attached directly to the sample as it is unable to withstand such high

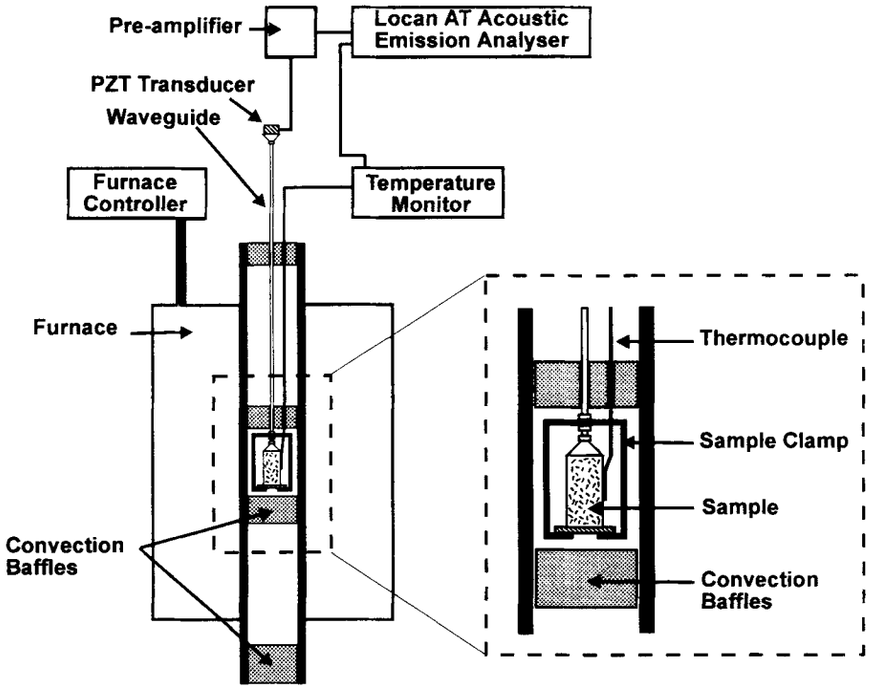

Figure 1. The acoustic-emission measurement arrangement.

temperatures. Instead, a waveguide was constructed out of high-temperature annealed stainless steel to allow the transducer to sit outside the furnace. The acoustic waveguide was designed to terminate in a 45° included angle cone at both ends. The AE transducer was bonded to the upper cone; the lower cone was clamped onto the sample by an annealed stainless-steel yoke. The use of this type of acoustic waveguide results in the loss of about 50 per cent of acoustic events due to absorption (Meredith & Atkinson 1983). Studies into the effect of using this type of waveguide have shown that, although the measured event rate is reduced, the shape of the event rate/amplitude distribution is unchanged, indicating that no preferential loss of events occurs in the amplitude range above an experimentally set threshold value. This is important because it means the use of this type of waveguide does not introduce systematic

Table 1. Description of samples. T_{qtz}, temperature at which the peak of acoustic-emission events associated with the quartz phase transition occurs. Q_{qtz}, Q values of the peak.

Sample	Rock Type	Origin	Average Grain Size	Composition	Max T /°C	T_{qtz}/°C	Q_{qtz}
DLB1	La Bresse Mylonite	Vosges (France)	10 μm	70.6% qtz, 15% feldspars, 6.2% hbl, 4.9% biotite, 3.3% muscovite	900	573.6	19
DLB2	La Bresse Mylonite	Vosges (France)	10 μm	70.5% qtz, 14% feldspars, 7.2% hbl, 4.8% biotite, 3.5% muscovite	900	573.1	22
KTB1	Amphibolite	KTB bore-hole 3656.7m	0.5 mm	59.2% qtz, 18.38% chl, 9.4% plag, 5.12% actinolite, 4.4% opaque oxides, 3.5% muscovite, trace biotite, apatite and epidote	900	573.0	36
KTB2	Hornblendeite	KTB bore-hole 3656.7m	0.5 mm	34.2% chl, 20.8% garnet, 19.2% actinolite, 15% plag, 5.2% opaque oxides, 4.4% muscovite, 1.2% qtz, trace biotite, apatite and epidote	875	none	n/a
KTB3	Amphibolite	KTB bore-hole 3656.7m	0.5 mm	42.97% qtz, 26.45% chl, 13.14% plag, 10% actinolite, 4.13% opaque oxides, 3.31% muscovite, trace biotite, apatite and epidote	950	574.1	28
LPG1	La Peyratte Granite	SE Armorican Massif (France)	1.5 mm	24% qtz, 35% plag, 29.3 Microcline, 4.7% muscovite, 7% biotite, trace apatite and rutile	625	572.3	28

errors into the measurement of peak amplitudes and b values (Meredith & Atkinson 1983).

Acoustic-emission signals from the transducer were amplified by 40 dB using a Panametrix low-noise pre-amplifier before analysis by a Locan AT acoustic-emission analyser. The acoustic-emission analyser was programmed to apply a further amplification of 42 dB and to accept data above a 26 dB threshold value. The level of the threshold value was set such that background noise would be eliminated from the recorded data. The acoustic-emission events (wave packets produced by a single event in the rock), counts (waves making up an event) and event amplitude were logged as a function of time and of temperature. The temperature was measured using a K-type thermocouple attached to the surface of the sample using a thick stainless-steel wire. Thermal baffles were inserted above and below the sample to reduce temperature gradients due to convection around the sample.

Acoustic emissions were monitored during tests in which the temperature of the sample was raised at 1 °C min^{-1} to a range of maximum temperatures (listed in Table 1). It is important that a distinction is made between cracks caused by thermal gradients within the sample and cracks induced purely as a result of anisotropic thermal expansion and thermal expansion mismatch between different minerals within the rock. A low rate of heating was used to ensure that all the cracking within the samples was due to thermal expansion, with no cracking due to thermal gradients. Typical thermal gradients during the experiments have been calculated as 0.9 °C cm^{-1}, equivalent to an average trans-grain temperature difference of less than 0.05 °C. This agrees well with experiments involving the cooling of granite below room temperature at 1 °C min^{-1}, which have shown temperature differences of 1 °C to 2 °C on 38 mm diameter samples (Meredith & Sammonds, private communication).

The acoustic-emission data were corrected to account for heat flow into the material and the subsequent temperature lag of the centre of the sample compared with that measured at its surface as well as the small temperature gradient occurring across the sample's length. A description of the samples, together with the measured temperature and Q value of the quartz transition AE peak, is given in Table 1. The Q value is defined here as the ratio of the height of the peak to its width at $1/e$ of its peak height, and is a measure of the sharpness of the peak.

The internal pore surface area of the connected porosity was measured with a nitrogen adsorption method on a Carlo Erba Sorptomatic 1900 (Brunauer, Emmet & Teller 1938). The amount of nitrogen molecules adsorbed onto the internal surface area of pores and cracks is a function of the temperature and pressure of the nitrogen gas in which the surface is immersed. The BET equation allows the volume of the adsorbed nitrogen molecules to be determined. The surface area associated with this adsorbed volume can be calculated providing the molecules are adsorbed in a monolayer and the effective surface area of a nitrogen molecule (A_e) is known ($A_e = 16.2\ A^2$).

Permeability measurements were performed with gas using the flux method based upon Darcy's Law. The measurements were corrected to take account of gas compressibility, inertia (Forchheimer effect), and molecular effects (Klinkenberg effect) where necessary (Debschutz, Kruckel & Schopper 1991; Darot, Gueguen & Baratin 1992).

2 RESULTS

Figures 2–4 show the combined acoustic emission, fluid permeability and surface area data on La Bresse mylonite, La Peyratte granite and KTB amphibolites, as a function of temperature.

The most striking feature shared by all of the acoustic-emission hit rate curves apart from that for KTB2 is the well-defined peak that occurs between 550 °C and 600 °C (Figs 2(a), 3(a) and 4). The peak in acoustic emissions has an average maximum for the five samples out of six in which it occurred of 573.2 ± 0.3 °C (see Table 1 for individual peak values). The peak is coincident with the α/β phase transition in quartz (573 °C). It is greatest in amplitude in the samples with the highest proportion of quartz (DLB1 and DLB2), and missing only in the sample that contained negligible amounts of that mineral (KTB2). We propose that the peak in acoustic-emission hit rate represents acoustic emissions that occur as a result of the gross microcracking induced by the stresses caused by increases in volume in quartz mineral grains during the phase transition. In addition, Reuschlé (1989) has shown that the surface energy of quartz becomes very low at the α/β phase transition by measuring the critical crack extension force versus temperature on quartz crystals using a double torsion method (Fig. 5). Consequently, cracking occurs very easily, and because so little energy is dissipated per unit length of new crack formation, many new cracks must be formed to enable the rock matrix to dissipate the deformation energy accumulated as stresses in the minerals while the temperature was rising toward the α/β phase transition temperature. One would expect, and indeed finds, that quartz grains undergo intensive crack nucleation at the phase transition temperature, which is exacerbated by a large difference in the thermal expansivities of β-quartz and feldspars at higher temperatures.

The production of a large number of new cracks should also have a large effect upon the absolute surface area of the rock, its porosity and its permeability to fluids. Measurements of absolute surface areas in La Peyratte granite (Fig. 2(b)) and La Bresse mylonite (Fig. 3(b)) show increases in the absolute internal surface area to a peak at about the α/β phase transition temperature. The decrease in pore surface area after the α/β phase transition temperature has been ascribed to the negative expansivity of β-quartz (Darot *et al.* 1992). Measurements of the fluid permeability of La Peyratte granite (Fig. 2(b)) and La Bresse mylonite (Fig. 3(b)) show large increases in fluid permeability in the temperature range 500–600 °C. The permeability of the La Peyratte granite increased by about two orders of magnitude between 500 and 600 °C compared with about a fivefold increase in the previous 100 °C rise in temperature. The increase in permeability has been ascribed to increased crack connectivity due to the addition of microcracks caused by the α/β phase transition, to new cracks and crack growth caused by the background differential thermal expansion, and anisotropy.

Measurements of the porosity of La Peyratte granite (Fig. 2(c)) also show a large increase in porosity at about the α/β

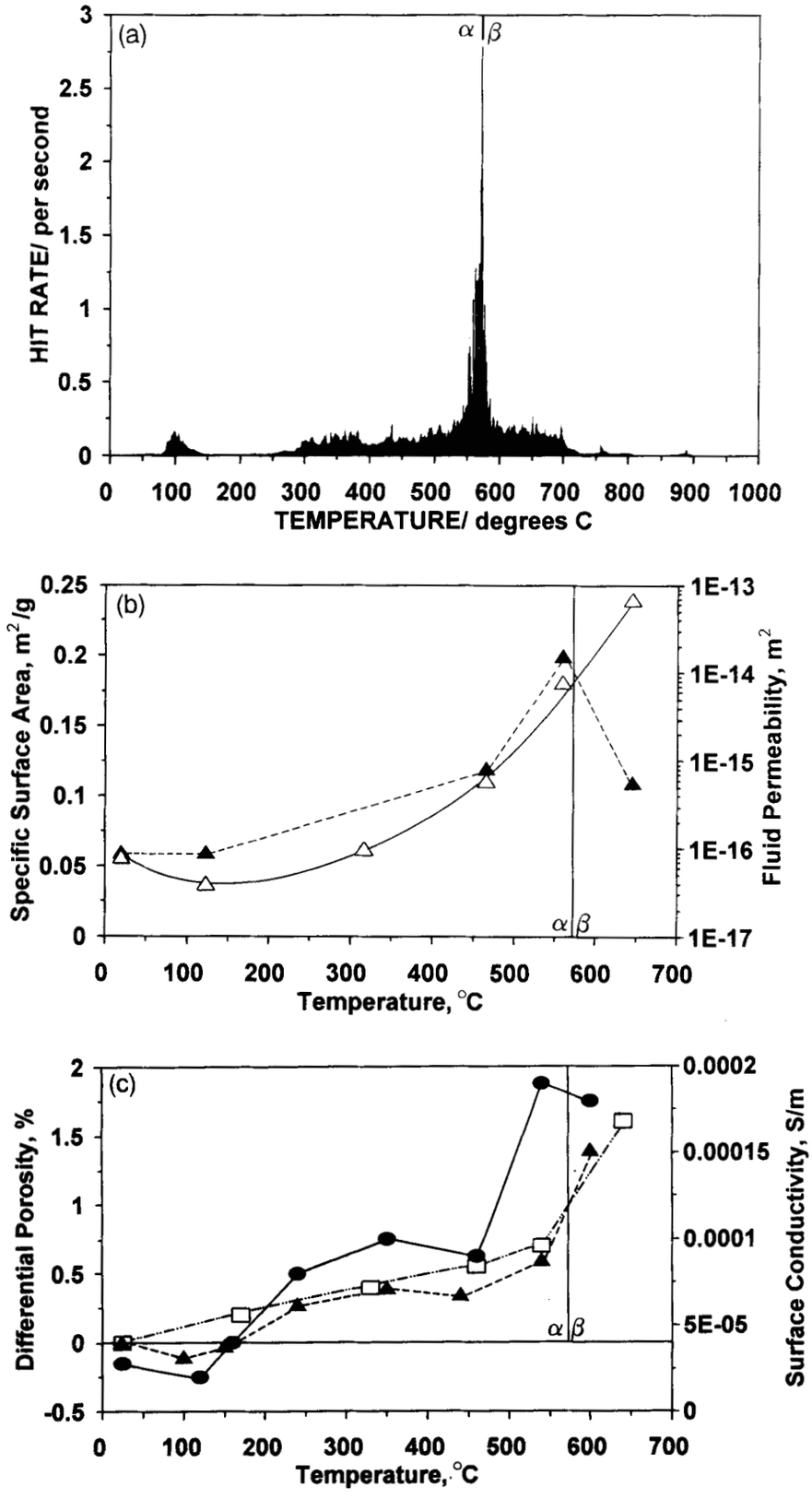

Figure 2. Measurements made upon samples of La Peyratte granite (LPG1). (a) The variation of acoustic-emission rate with temperature; (b) the variation of BET total internal surface area (solid triangles) (after C. Ruffet 1993), and fluid permeability (open triangles) with heat treatment temperature; (c) the variation of porosity relative to that at 20 °C for two samples (solid triangles and open squares), and surface conductivity for samples containing initially deionized water (solid circles) (after C. Ruffet 1993), with heat treatment temperature.

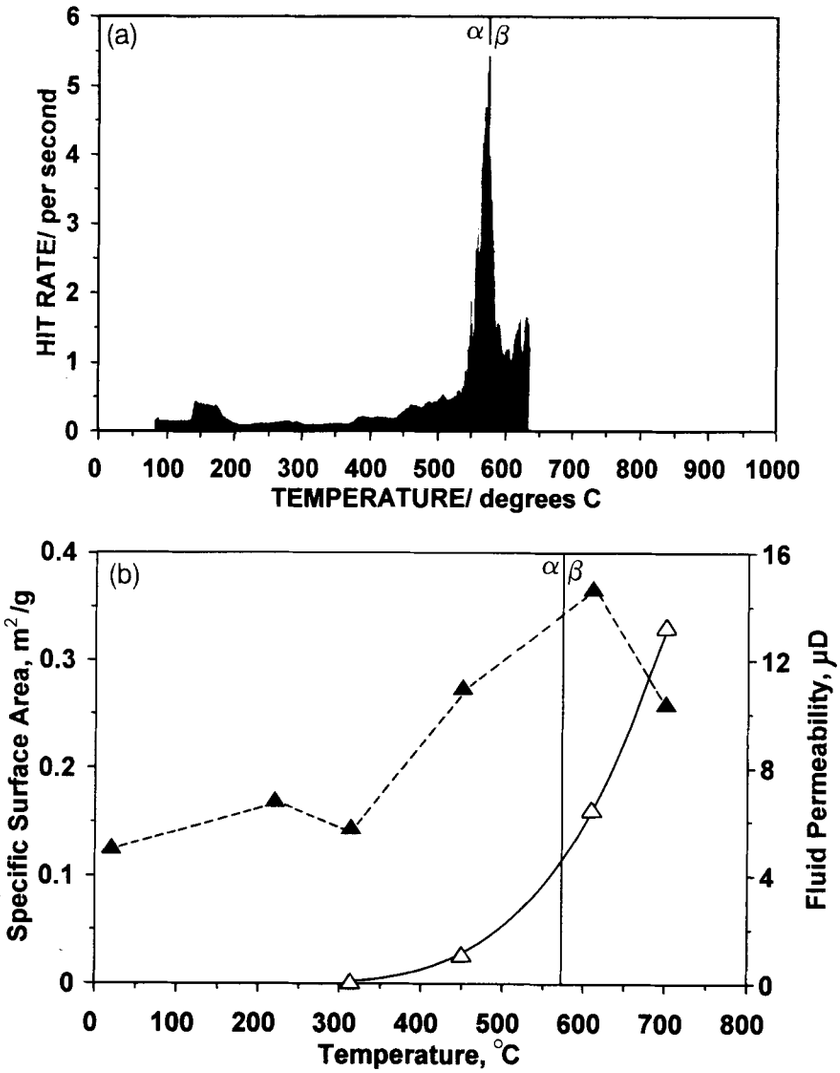

Figure 3. Measurements made upon samples of La Bresse mylonite (DLB1 and DLB2). (a) The variation of acoustic-emission rate with temperature, and (b) the variation of BET total internal surface area (solid triangles) and fluid permeability (open triangles) with heat treatment temperature.

phase transition temperature. Measurements of the surface conductivity of samples of rock that had been previously heat treated to various maximum temperatures have also been done. Surface conductivity was measured by ascertaining the electrical conductivity of the rock when saturated with very weak electrolytes, when it can be assumed that electrical conduction through the body of the fluid occupying the cracks and pores is negligible compared with the conduction occurring over the surface of grains due to the hopping migration of ions. The surface conduction is, therefore, another measure of the crack and pore surface area, and would be expected to increase as cracking occurs and new cracks are formed. Surface conductivity measurements for La Peyratte granite (Fig. 2(c)) show increases that mirror the absolute surface area measurements obtained by the BET method (Fig. 2(b)), doubling in size between about 450 °C and 600 °C, indicating a large increase in the amount of crack surface area at temperatures around the α/β phase transition temperature.

Finally, the extensive crack system produced by microcracking consequent upon the α/β phase transition was also observed using electron and optical microscopy (Fig. 6).

The amplitude distribution of acoustic-emission events is commonly characterized by the microseismic b value which is defined by the equation

$$v(A) = \left(\frac{A}{A_o}\right)^{-b} \tag{1}$$

where $v(A)$ is the fraction of the emission set whose amplitude exceeds amplitude A, and A_o is the lowest detectable amplitude. A small value of b indicates that a population of acoustic events has a large proportion of high-amplitude events, while a large value of b indicates that smaller-amplitude events predominate. Large decreases in b can be observed during the deformation of rocks to failure, as microcracks increase in size until a macroscopic fracture zone is produced (Sammonds, Meredith & Main 1992).

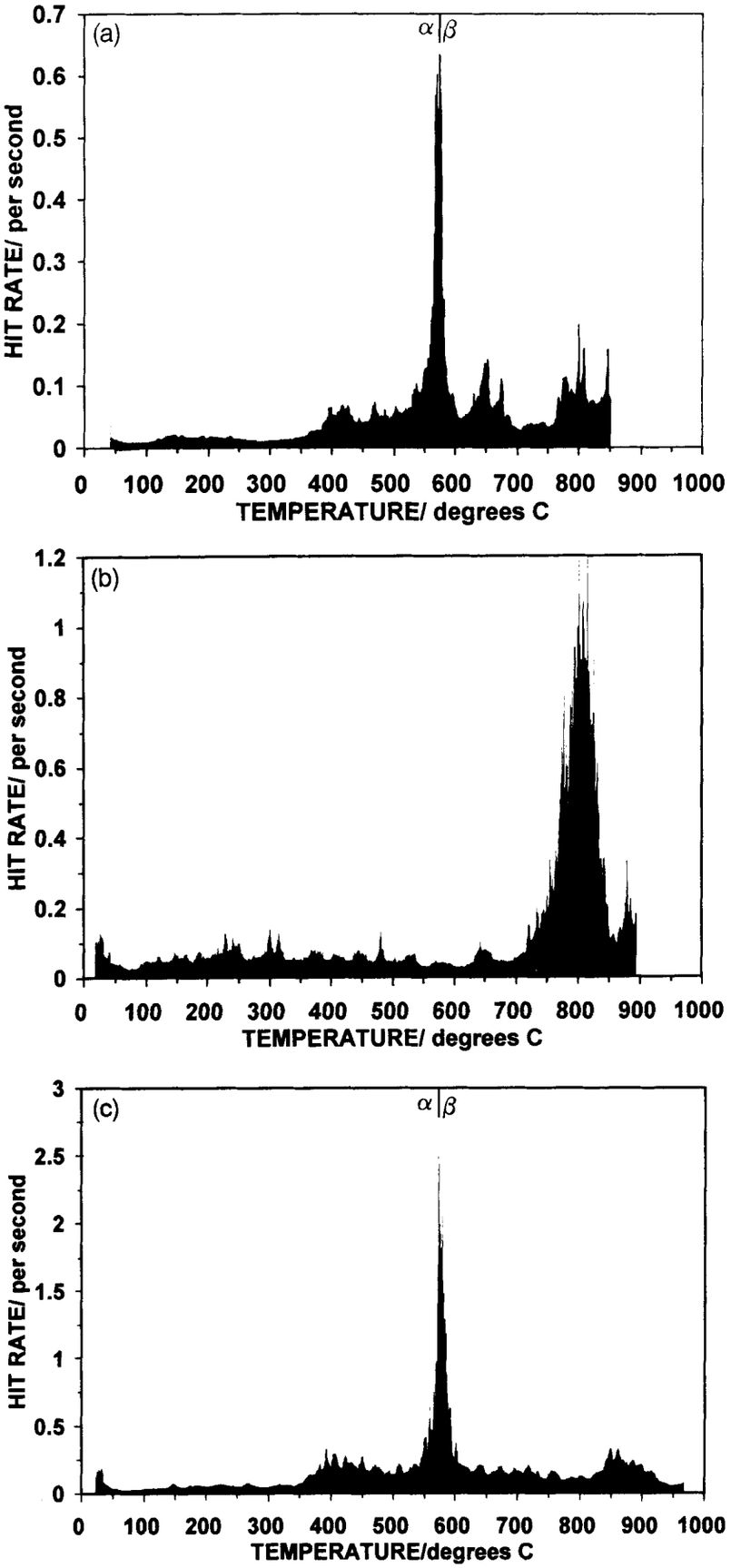

Figure 4. Measurements made upon samples of KTB amphibolite: (a) KTB1, (b) KTB2, (c) KTB3, showing the variation of acoustic-emission rate with temperature for each sample.

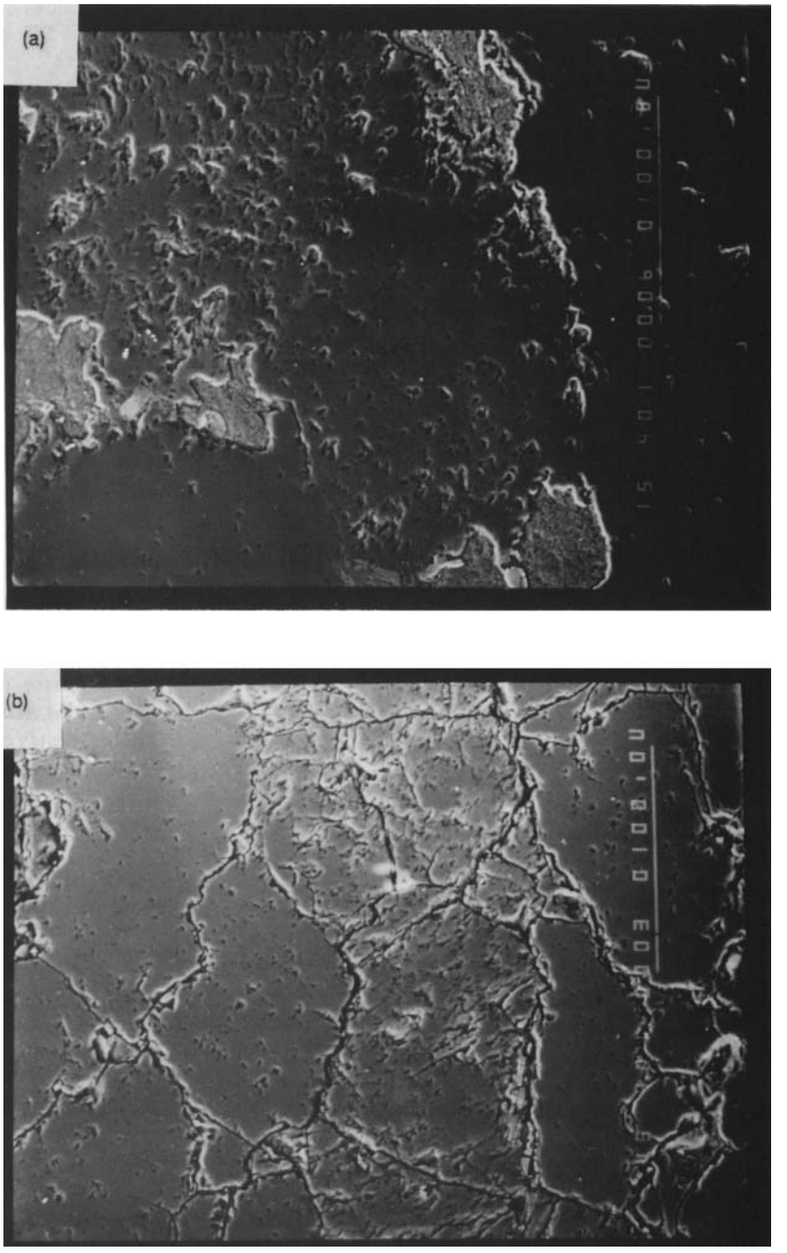

Figure 6. Optical/SEM micrographs of typical sections of KTB amphibolite (KTB3) (a) before and (b) after heat treatment above the quartz α/β phase transition temperature (magnification 400×).

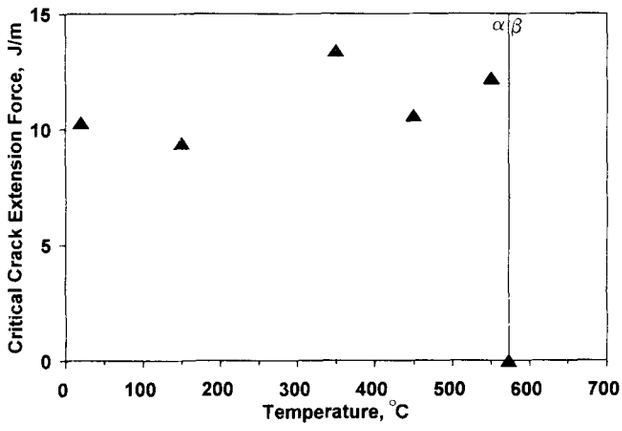

Figure 5. Critical crack extension force versus temperature. Data obtained from double torsion experiments on quartz single crystals (after T. Reuschlé 1989).

Microcracks occurring as a result of background differential thermal expansion and anisotropy would be expected to be constrained by their interaction with the grain boundaries, resulting in a predominance of small events, and consequently a high b value which remains constant as the temperature is raised. A slight decrease in the b value has been observed by some researchers as the temperature is raised, indicating a small increase in the number of higher-amplitude events at higher temperatures (Atkinson *et al.* 1984).

Microcracks occurring as a response to the α/β phase transition would not be expected to cause a decrease in the b value, because, although the rate of microcrack formation might be inferred to increase greatly from the observed peak of acoustic-emission hit rate, the amplitude of the acoustic-emission population as a whole will remain constrained by the grain size. It is, therefore, most likely that the b value will remain constant throughout the phase transition. Calculation of b values from our experiments showed that the values remained constant through the phase transition as expected.

Sample KTB2 failed to give an AE peak at the quartz phase transition temperature, and was found to contain negligible amounts of quartz. Although listed as a KTB amphibolite, it was predominantly composed of retrogressed chlorite with metal oxides which underwent an oxidation–dehydroxylation reaction to oxy-hornblende at about 800 °C. This reaction resulted in a clear peak in acoustic emissions centred around this temperature. The peak was also present but to a lesser extent in samples DLB1, DLB2, KTB1 and KTB3, all of which contained smaller proportions of chlorite or hornblende, which undergoes a similar dehydroxylation reaction at this temperature. We envisage the acoustic emissions occurring due to microcrack nucleation as a result of differences in the specific volumes of the reactants and the products of the geochemical reaction. It is interesting to note that the acoustic-emission hit rate peak produced by this mechanism is much broader than that associated with the α/β phase transition; we have interpreted this as being due to the larger reaction time of the chemical reaction which depends upon the diffusion of ions through the mineral lattices, compared with the physical process of the α/β phase transition which is a physical discontinuity whose measured width depends only upon the heat transfer within the sample.

It is interesting to note that the acoustic-emission rate is still significant at temperatures higher than 800 °C. The mechanism for these events is not necessarily brittle failure producing microcracks; rather the explosion of fluid inclusions and dehydroxylation reactions producing gaseous fluids at high temperatures. If this is the case the rock may produce acoustic emissions whilst behaving in a very plastic manner with mass distribution occurring by partial melting and recrystallization along grain boundaries.

3 CRUSTAL IMPLICATIONS

The recognition that gross microcracking can occur in rocks as a result of the phase transitions in quartz has implications for the electrical conductivity of the Earth's continental lower crust. The presence of highly conducting zones in the lower crust is still one of the most elusive riddles preventing the full geological understanding of the Earth's continental crust. The majority of these zones occur at depths between 20 and 30 km, which represents a temperature range of 400–600 °C in most Phanerozoic regions. Numerous sources of the electrical conductivity have been proposed such as aqueous fluids from various sources (Hyndman & Shearer 1989; Marquis & Hyndman 1992), graphite films (e.g. Glover & Vine 1992), and other conductive minerals and partial melt (Hermance 1979), together with controlling factors such as the presence of lower crustal shear zones (Brodie & Rutter 1987; Marquis & Hyndman 1992) and the brittle–ductile behaviour of rock at depth (Gough 1986; Marquis & Hyndman 1992). It is likely that the variability in the characteristics of lower crustal high-conductivity zones from region to region is due to the operation of different mechanisms. We suggest that in some regions where progradational conditions are present, or rocks are being carried to depth associated with subduction, and where high electrical conductivities are due to aqueous fluids, the high lateral connectivity required may be provided by microcracking consequent upon the α/β phase transition in quartz. It is important to note, however, that the behaviour observed in this study was observed in dry rocks under no confining pressure, or chemical control. Such a hypothesis could only be seriously considered if experiments on saturated rocks at raised confining pressure and pore-fluid pressure also produced clear peaks of microcracking. The presence of an electrolyte may contribute to greater microcracking resulting from stress corrosion (Meredith & Atkinson 1985). Alternatively, the presence of aqueous fluids in the pore space may cause the rock to behave in a ductile fashion by 573 °C allowing the volume change associated with the quartz phase transition to be accommodated by plastic deformation without the formation of thermally induced cracks.

4 CONCLUSIONS

This work has confirmed previous studies that have shown that slow heating of rock samples in air at atmospheric pressure produces microcracks as a result of anisotropic mineral expansion and multimineral differential thermal

expansion. In addition, quartz-bearing rock samples which have been slowly heated through the α/β quartz phase transition undergo gross microcracking as a result of the sudden volumetric expansion that occurs during the phase transition and the release of strain energy accumulated in confined minerals when the surface energy becomes very low at the phase transition. These microcracks can be monitored as they occur using acoustic-emission monitoring techniques. Acoustic-emission techniques are not only useful to monitor microcracks caused by the phase transition but can also monitor the occurrence of other processes producing short-period releases of energy within the rock such as the explosion of fluid inclusions.

ACKNOWLEDGMENTS

We thank the staff of the Haskel Laboratory, UCL, UK, and the Petrophysics Laboratory, TU Clausthal, Germany, where some of this work was performed. We also thank J. Baker and L. Martin of the Rock and Ice Physics Laboratory, UCL, UK; Clothilde Ruffet of EOPGS, Strasbourg, France, for assisting with some measurements, and D. Pribnow for providing the KTB samples. This work was made possible with the financial support from the British Council/French Government under the ALLIANCE programme, the French and German governments under the PROCOPE programme, and the NERC Research Grant GR3/8289. This paper is Contribution 53 of the Research School of Geological and Geophysical Sciences, University College, London, UK.

REFERENCES

Atkinson, B.K., McDonald, D. & Meredith, P.G., 1984. Acoustic response and fracture mechanics of granite subjected to thermal and stress cycling experiments, in *Proc. 3rd Int. Conf. on Acoustic Emission/Microseismic Activity in Geological Structures and Materials*, pp. 5–18, eds Hardy, H.R. & Lieghton, F.W., Trans-Tech, Clausthal, Germany.

Brodie, K.H. & Rutter, A.H., 1987. Deep crustal extensional faulting in the Ivrea Zone of northern Italy, *Tectonophysics*, **140,** 193–212.

Brunauer, S., Emmet, P.H. & Teller, E., 1938. Adsorption of gasses in multi-molecular layers, *J. Am. Chem. Soc.*, **60,** 309–319.

Darot, M., Gueguen, Y. & Baratin, M., 1992. Permeability of thermally cracked granite, *Geophys. Res. Lett.*, **19** (9), 869–872.

Debschutz, W., Kruckel, U. & Schopper, J.R., 1991. Measurements of the hydraulic flow properties of crystalline rocks to characterize the internal pore-space structure, *Scientific Drilling*, **2,** 58–66.

Friedman, M. & Johnson, B., 1978. Thermal cracks in unconfined sioux granite, *Proc. US Symp. Rock Mech.*, **19,** 423–430.

Friedrich, J.T. & Wong, T., 1986. Micromechanics of thermally induced cracking in three crustal rocks, *J. geophys. Res.*, **91** (B12), 12 743–12 764.

Glover, P.W.J. & Vine, F.J., 1992. Electrical conductivity of carbon-bearing granulite at raised temperatures and pressures, *Nature*, **360,** 723–726.

Gough, D.I., 1986. Seismic reflectors, conductivity, water and stress in the continental crust, *Nature*, **323,** 143–144.

Hermance, J.F., 1979. The electrical conductivity of materials containing partial melt, *Geophys. Res. Lett.*, **6,** 613–616.

Homand-Etienne, F. & Troalan, J.-P., 1984. Behaviour of granites and limestone subjected to slow and homogeneous temperature changes, *Eng. Geol.*, **20,** 219–233.

Hyndman, R.D. & Shearer, P.M. 1989. Water in the lower continental crust: modelling magnetotelluric and seismic reflection results, *Geophys. J. Int.*, **98,** 343–365.

Marquis, G. & Hyndman, R.D., 1992. Geophysical support for aqueous fluids in the deep crust: seismic and electrical relationships, *Geophys. J. Int.*, **110,** 91–105.

Meredith, P.G. & Atkinson, B.K., 1983. Stress corrosion and acoustic emission during tensile crack propagation in Whin Sill dolerite and other basic rocks, *Geophys. J. astr. Soc.*, **75,** 1–21.

Meredith, P.G. & Atkinson, B.K., 1985. Fracture toughness and subcritical crack growth during high temperature tensile deformation of Westerly Granite and Black Gabbro, *Phys. Earth planet. Inter.*, **39,** 33–51.

Reuschlé, T., 1989. Les fluides et l'evolution des proprietes mechaniques des roches, *PhD Thesis,* Louis Pasteur University, Strasbourg.

Ruffet, C., 1993. La conductivite electrique complexe dans quelques roches crustales, *PhD Thesis,* Louis Pasteur University, Strasbourg.

Sammonds, P.R., Meredith, P.G. & Main, I., 1992. Role of pore fluids in generation of seismic precursors to shear fracture, *Nature*, **359,** 228–230.

Simmons, G. & Cooper, H.W., 1978. Thermal cycling cracks in three igneous rocks, *Int. J. Rock Mech. Min. Sci.*, **15,** 145–148.